

# A Fast Inversion Method for Interpreting Crosshole Electromagnetic Data

Hee Joon Kim<sup>1)</sup>, Ki Ha Lee<sup>2)</sup> and Michael J. Wilt<sup>3)</sup>

1) Pukyong National University, Busan 608-737, Korea

2) Ernest Orlando Lawrence Berkeley National Laboratory, Berkeley, CA 94720, U. S. A.

3) ElectroMagnetic Instruments, Inc., Richmond, CA 94804, U. S. A.

**Abstract:** The extended Born or localized nonlinear (LN) approximation of integral equation (IE) solutions has been applied to inverting crosshole EM data using a cylindrically symmetric model. The LN approximation is less accurate than a full solution but much superior to the simple Born approximation. Moreover, when applied to the cylindrically symmetric model with a vertical magnetic dipole source, the LN approximation works well because electric fields are scalar and continuous everywhere. One of the most important steps in the inversion is the selection of a proper regularization parameter for stability. The LN solution provides an efficient means for selecting an optimum regularization parameter, because Green's functions, the most time consuming part in IE methods, are repeatedly re-usable throughout the selection process. In addition, the IE formulation readily contains a sensitivity matrix, which can be revised at each iteration at little expense. This fast inversion scheme has been tested on its stability and efficiency using synthetic and field data.

## 1. Introduction

High-resolution imaging of electrical conductivity has been the subject of many studies in crosshole tomography using electromagnetic (EM) fields (Zhou et al., 1993; Wilt et al., 1995; Alumbaugh and Morrison, 1995; Newman, 1995; Alumbaugh and Newman, 1997). Although the theoretical understanding and associated field practices for crosshole EM methods are relatively mature, fast and stable interpretation of crosshole EM data is still a challenging problem.

The main advantage of integral equation (IE) method in comparison with the finite difference (FD) and/or finite element (FE) method is the fast and accurate simulation of compact three-dimensional (3-D) bodies in a layered background (Hohmann, 1975). The FD and FE methods are suitable for modeling EM fields in complex structures with large-scale conductivity variations. In principle, the IE method can handle these models too, but the huge demand on computer resources places a practical limit on its use. This is because of the full matrix arising from the IE formulation.

Another advantage of the IE method over the FD or FE method is its greater suitability for inversion. The IE formulation readily contains a sensitivity matrix, which can be revised at each

inversion iteration at little expense. With the FD or FE method, in contrast, the sensitivity matrix has to be recomputed at each iteration at a cost nearly equal to that of full forward modeling. The IE method, however, has to overcome severe practical limitations imposed on the numerical size of the anomalous domain for inversion purposes. In this direction, several approximate methods such as the extended Born or localized nonlinear (LN) approximation (Habashy et al., 1993) and quasi-linear approximation (Zhdanov and Fang, 1996) have been developed recently.

In this paper we exploit an advantage of the LN approximation with applications to crosshole inversion of EM data. We begin our discussion with a review of the LN approximation of IE solutions. We then consider its accuracy for a cylindrically symmetric model, describe our inversion algorithm, and demonstrate the stability and effectiveness of this approach by inverting synthetic data. Finally, we briefly consider an example application to field data provided by Chevron as a part of the Lost Hills CO<sub>2</sub> pilot project in southern California.

## 2. LN approximation

Assuming an  $e^{+i\omega t}$  time dependency and neglecting displacement currents, an IE solution for the electric field  $\mathbf{E}(\mathbf{r})$  at  $\mathbf{r}$  can be written by (Hohmann, 1975)

$$\mathbf{E}(\mathbf{r}) = \mathbf{E}_b(\mathbf{r}) - i\omega \oint_V \mathbf{G}_E(\mathbf{r} - \mathbf{r}') \cdot \Delta \mathbf{S}(\mathbf{r}') \mathbf{E}(\mathbf{r}') dV', \quad (1)$$

where  $\mathbf{E}_b(\mathbf{r})$  is the background electric field,  $\mathbf{G}_E(\mathbf{r} - \mathbf{r}')$  the Green's tensor,  $\mathbf{S}$  the conductivity,  $\omega$  the angular frequency, and  $\mu$  the magnetic permeability. In equation (1),  $\Delta \mathbf{S}$  means the excess conductivity, and the term  $\Delta \mathbf{S} \mathbf{E}$  inside the integral is called the scattering current (Hohmann, 1975). To obtain a numerical solution, the anomalous body is usually divided into a number of cells, and a constant electric field is assigned to each cell (Hohmann, 1988). The process involved in volume IE methods requires computing time proportional to the number of cells used, and it quickly becomes impractical as the size of the inhomogeneity is increased to handle realistic problems.

For some important class of problems the complexity associated with a full 3-D problem can be reduced to something much simpler. A model whose electrical conductivities are cylindrically symmetric in the vicinity of a borehole is such an example. In order to preserve the cylindrical symmetry in the resulting EM fields, a horizontal loop current source or a vertical magnetic dipole may be considered in the borehole. In this case the problem is scalar when formulated using the azimuthal electric field  $E_\phi$ , and the analogous IE solution is

$$E_j(\mathbf{r}) = E_{jb}(\mathbf{r}) - 2\pi i \omega \mathbf{m} \iint_{\mathbf{r}z} G_E(\mathbf{r} - \mathbf{r}') \Delta \mathbf{S}(\mathbf{r}') E_j(\mathbf{r}') \mathbf{r}' d\mathbf{r}' dz', \quad (2)$$

where  $\mathbf{r} = \bar{\mathbf{r}} + \bar{z}$  and  $\mathbf{r}' = \bar{\mathbf{r}}' + \bar{z}'$  are the position vectors, and the electric field and Green's function are both scalar. The Green's function is given in the form of a Hankel transform as (p. 219, Ward and Hohmann, 1988)

$$G_E(\mathbf{r} - \mathbf{r}') = -\frac{1}{4\pi} \int_0^\infty \frac{e^{-u_b|z-z'|}}{u_b} \mathbf{I} J_1(\mathbf{I} \mathbf{r}) J_1(\mathbf{I} \mathbf{r}') d\mathbf{I}, \quad (3)$$

where  $u_b = (\mathbf{I}^2 + i\omega \mathbf{m}_b)^{1/2}$ . Since measurements are usually made for the magnetic field, equation (2) is modified as

$$H_z(\mathbf{r}) = H_{zb}(\mathbf{r}) - 2\pi i \omega \mathbf{m} \iint_{\mathbf{r}z} G_H(\mathbf{r} - \mathbf{r}') \Delta \mathbf{S}(\mathbf{r}') E_j(\mathbf{r}') \mathbf{r}' d\mathbf{r}' dz', \quad (4)$$

where  $G_H(\mathbf{r} - \mathbf{r}')$  translates the scattering current  $\Delta \mathbf{S}(\mathbf{r}') E_j(\mathbf{r}')$  at  $\mathbf{r}'$  to the magnetic field at  $\mathbf{r}$ .

Using equations (2) through (4), we can obtain an IE solution by first dividing the  $(\mathbf{r}; z)$  cross-section into a number of cells, and formulate a system of equations for the electric field using a pulse basis function. Sena and Toksoz (1990) presented a crosshole inversion study for permittivity and conductivity in cylindrically symmetric medium using high-frequency EM, and Alumbaugh and Morrison (1995) investigated crosshole EM tomography using an iterative Born approximation.

The LN approximation offers an efficient and reasonably accurate electric field solution without deriving the full IE solution (Habashy et al., 1993). For the type of problem where there is only the azimuthal electric field, a good LN approximation to equation (2) is given by

$$E_j(\mathbf{r}) \approx \mathbf{g}(\mathbf{r}) E_{jb}(\mathbf{r}), \quad (5)$$

where

$$\mathbf{g}(\mathbf{r}) = \left[ 1 + 2\pi i \omega \mathbf{m} \iint_{\mathbf{r}z} G_E(\mathbf{r} - \mathbf{r}') \Delta \mathbf{S}(\mathbf{r}') \mathbf{r}' d\mathbf{r}' dz' \right]^{-1}.$$

Substituting equation (5) into equation (4), we get an approximate magnetic field solution

$$H_z(\mathbf{r}) = H_{zb}(\mathbf{r}) - 2\pi i \omega \mu \iint_{\mathbf{r}z} G_H(\mathbf{r} - \mathbf{r}') \Delta \mathbf{S}(\mathbf{r}') \mathbf{g}(\mathbf{r}') E_{jb}(\mathbf{r}') \mathbf{r}' d\mathbf{r}' dz'. \quad (6)$$

To illustrate the efficiency and usefulness of the LN numerical solution, especially in a crosshole application, let us consider a simple model consisting of a conductive ring about a source borehole axis in a uniform whole space of 100 ohm-m. The cross-section of the ring is a 10 m by 10 m rectangle and 15 m horizontally away from the borehole as shown in Figure 1. The Born and LN approximated magnetic fields measured in the other borehole 50 m horizontally away from the source borehole are compared with the result obtained from the full FE method (Lee et al., 2002).

Figure 2 shows the comparison in the secondary horizontal and vertical magnetic fields between the Born, LN, and FE solutions. The center of the body is chosen as  $z = 0$ . The conductivity contrast and operating frequency used are 10 and 10 kHz, respectively. The source and receiver are located at the same depth in each borehole. More anomalies can be observed in the imaginary part than in the real part. For all field components, the LN and FE solutions agree very well.

We are also interested in the quality of the LN solution when the conductivity of the body is varied. Figure 3 shows the comparison in the secondary vertical magnetic fields between the Born, LN, and FE solutions. A vertical magnetic source is fixed at the depth of the center of body in the source borehole, and vertical magnetic fields are measured at 10 m below the center of the body in the receiver borehole. The frequency used is 10 kHz. The LN approximation is very well up to the conductivity contrast of about 100. The imaginary part of the LN solution starts deviating from the FE solution beyond the conductivity contrast of 100, while the real part still shows a good agreement.

Finally, the comparison is made for responses in frequency as shown in Figure 4. The source-receiver array is the same as that in Figure 3, and the conductivity contrast is fixed to 10. The LN and FE solutions show a good agreement all the way up to about 100 kHz.

### 3. Inversion

Based on the encouraging results of the LN approximation, we have proceeded to implement the crosshole EM inversion. Measurements are in the other borehole to the transmitter borehole. Upon dividing the inhomogeneity into  $K$  elements, the secondary magnetic field at the  $i$ -th receiver in the borehole may be written as

$$H_{zi}^s \approx -2\pi\omega\mu\sum_{k=1}^K \Delta\mathbf{s}_k \mathbf{g}_k E_{jbk} \iint_{S_k} G_H(\mathbf{r}', z_i - z') \mathbf{r}' d\mathbf{r}' dz', \quad (7)$$

where the subscript  $k$  denotes the  $k$ -th element. The corresponding Green's function for the magnetic field may be deduced from the electric field Green's function (3) as

$$G_H(\mathbf{r}', z_i - z') = \frac{1}{4\pi\omega\mu_0} \int_0^\infty \frac{e^{-u_b|z-z'|}}{u_b} \mathbf{I}^2 J_1(\mathbf{I}\mathbf{r}') d\mathbf{I}. \quad (8)$$

For the inversion, the sensitivity of the magnetic field with respect to the change in conductivity can be easily obtained from equation (7). Taking derivative of the data with respect to the  $j$ -th conductivity parameter and neglecting the dependence of  $\mathbf{g}$  on  $\Delta\mathbf{S}$ , the sensitivity becomes

$$\frac{\partial H_{zi}^s}{\partial \mathbf{s}_j} \approx -2\pi\omega\mu\mathbf{g}_j E_{jbj} \iint_{S_j} G_H(\mathbf{r}', z_i - z') \mathbf{r}' d\mathbf{r}' dz', \quad (9)$$

which can be easily evaluated by integrating over the  $j$ -th element.

The inversion procedure starts with the data misfit  $\|\mathbf{W}_d[\mathbf{H}(\mathbf{s}) - \mathbf{H}_d]\|^2$ , where the subscript  $d$  denotes data. The data weighting matrix  $\mathbf{W}_d$  is used to give relative weights to individual data. If a perturbation  $d\mathbf{s}$  is allowed to the conductivity, the misfit takes a form  $\|\mathbf{W}_d[\mathbf{H}(\mathbf{s} + d\mathbf{s}) - \mathbf{H}_d]\|^2$ , and the total objective functional may be written as

$$\mathbf{f} = \|\mathbf{W}_d[\mathbf{H}(\mathbf{s} + d\mathbf{s}) - \mathbf{H}_d]\|^2 + \mathbf{I} \|\mathbf{W}_s d\mathbf{s}\|^2, \quad (10)$$

where the second term on the right-hand side is added to impose a smoothness constraint, and  $\mathbf{W}_s$  is the weighting matrix and  $\mathbf{I}$  is the Lagrange multiplier that controls the trade-off between data misfit and parameter smoothness. Expanding the misfit in  $d\mathbf{s}$  using the Taylor series, discarding terms higher than the square term, and letting the variation of the functional with respect to  $d\mathbf{s}$  equal to zero, we obtain a linear system of equations for the perturbation  $d\mathbf{s}$  as

$$(\mathbf{J}^T \mathbf{W}_d^T \mathbf{W}_d \mathbf{J} + \mathbf{I} \mathbf{W}_s^T \mathbf{W}_s) d\mathbf{s} = -\mathbf{J}^T \mathbf{W}_d^T \mathbf{W}_d [\mathbf{H}(\mathbf{s}) - \mathbf{H}_d], \quad (11)$$

where the superscript  $T$  indicates the matrix transpose, and the entries of Jacobian matrix  $\mathbf{J}$  are the sensitivity functions given in equation (9).

The stability of the inversion is largely controlled by requiring the conductivity to vary smoothly. Larger values of  $\mathbf{I}$  result in smooth and stable solutions at the expense of resolution. It even allows for the solution of grossly underdetermined problems (Tikhonov and Arsenin, 1977). In this crosshole inversion study, we employ the Occam approach, first proposed by Constable et al. (1987) (see also deGroot-Hedlin and Constable, 1990; Parker, 1994), to determine an optimum Lagrange multiplier  $\mathbf{I}$  during the inversion process. The unique feature of the Occam approach is that the parameter  $\mathbf{I}$  is used in each iteration both as a step length control and a smoothing parameter. That is, equation (16) is solved for a series of trial values of  $\mathbf{I}$  and the rms misfit for each  $\mathbf{I}$  is evaluated by solving the 2-D forward problem. The Occam process thus chooses the model with the minimum misfit as the basis for the next iteration. The minimization can be carried out by means of a simple 1-D line search. In this selection scheme, the IE modeling is quite attractive in speed because Green's functions, the most time consuming part in IE methods, are repeatedly re-usable throughout the selection procedure.

To evaluate the performance of extended Born inversion using the LN approximation, we choose a conductivity model shown in Figure 5. The model consists of two cylindrically symmetric bodies, one conductive (0.1 S/m) and the other resistive (0.001 S/m), in a whole space of 0.01 S/m. A FE scheme (Lee et al., 2002) is used to generate synthetic data. The accuracy of the FE method is estimated as a level of less than 1 %. Using a vertical magnetic dipole ( $M_z$ ) as a source, vertical magnetic fields ( $H_z$ ) are computed at three frequencies of 2.5 kHz, 10 kHz and 20 kHz. Three-percent Gaussian noise is added to the synthetic data prior to the inversion. The inversion is started with an initial model of 60 ohm-m uniform whole space. In this test three forward modelings are performed to select an optimum Lagrange multiplier in each iteration.

After 8 iterations, the two bodies are clearly reconstructed as shown in Figure 6. The recovered conductivity is found to be nearly the same in the conductive body but is overestimated in the resistive body. The inversion process is quite stable, and the rms misfit decreases from the initial guess of 5.095 to 0.036 after 8 iterations. The smoothing parameter varies significantly during the inversion process. This means it is difficult to determine the parameter a priori.

Finally, the 2-D inversion algorithm has been applied to a set of crosshole field data provided by Chevron as a part of the Lost Hills CO<sub>2</sub> pilot project in southern California (Wilt, 2002). The separation between the two vertical boreholes is 24.536 m and CO<sub>2</sub> injection well is near the center of the section defined by the two wells. Although both EM and seismic data for the pre- and post-injection are available, we conducted inversion using only the EM ( $M_z$ - $H_z$ ) data. The operating frequency was 759 Hz.

Figure 7 shows inversion results of the crosshole data. The CO<sub>2</sub> injection into a reservoir of oil/brine mixture results in changes in conductivity, which can be indirectly interpreted as the displacement of brine with injected CO<sub>2</sub>. The replacement of water with CO<sub>2</sub> makes a decrease of conductivity. Figure 7 shows a significant change in resistivity distribution, and this increase of resistivity suggests an effect of the CO<sub>2</sub> injection. Unfortunately, the borehole separation is not far enough compared with the skin depth (i.e., low frequency), the reconstructed images using the assumption of cylindrically symmetry may have artifacts that can be produced by the geometry of conductive zone outside of the interwell plane (Alumbaugh and Morrison, 1995). Computing time required for the 2-D approximate inversion is less than 5 minutes on a Pentium-4 PC to obtain 650 conductivities from 604 complex  $H_z$  fields after 5 iterations.

#### 4. Conclusions

A computationally efficient inversion scheme has been developed using the LN approximation to analyze electromagnetic fields obtained in a crosshole environment. The medium is assumed to be cylindrically symmetric about the borehole, and to maintain the symmetry vertical magnetic dipole source is used as a source. The efficiency and robustness of an inversion scheme is very much dependent on the proper use of Lagrange multiplier, which is often provided manually to achieve a desired convergence. We have employed an automatic Lagrange multiplier selection scheme, which enhances the utility of the inversion scheme in handling field data. In this selection scheme, the IE method is quite attractive in speed because Green's functions, the most time consuming part in IE methods, are repeatedly re-usable throughout the selection procedure. The inversion scheme using the LN approximation has been tested to show its stability and efficiency using synthetic and field data.

This work was supported by the Assistant Secretary for Energy Efficiency and Renewable Energy, Office of Wind and Geothermal Technologies of the U.S. Department of Energy under Contract No. DE-AC03-76SF00098. We would like to thank Michael Morea, Chevron USA Production Company, and the US Department of Energy, National Petroleum Technology Office, (Class III Field Demonstration Project DE-FC22-95BC14938) for allowing us to publish this data. Korea Science and Engineering Foundation (R01-2001-000071-0) provided support for this study.

#### References

Alumbaugh, D. L. and Morrison, H.F., 1995, Theoretical and practical considerations for crosswell electromagnetic tomography assuming a cylindrical geometry, *Geophysics*, **60**, 846-870.

- Alumbaugh, D. L., and Newman, G. A., 1997, Three-dimensional massively parallel electromagnetic inversion—II. Analysis of crosswell electromagnetic experiment, *Geophys. J. Int.*, **128**, 355-363.
- Constable, S. C., Parker, R. L., and Constable, C. G., 1987, Occam's inversion: A practical algorithm for generating smooth models from electromagnetic sounding data, *Geophysics*, **52**, 289-300.
- deGroot-Hedlin, C. and Constable, S., 1990, Occam's inversion to generate smooth, two-dimensional models from magnetotelluric data, *Geophysics*, **55**, 1613-1624.
- Habashy, T. M., Groom, R. M., and Spies, B. R., 1993, Beyond the Born and Rytov approximations: a nonlinear approach to electromagnetic scattering, *J. Geophys. Res.*, **98**, 1795-1775.
- Hohmann, G. W., 1975, Three-dimensional induced polarization and EM modeling, *Geophysics*, **40**, 309-324.
- Hohmann, G. W., 1988, Numerical modeling for electromagnetic methods of geophysics, in Nabighian, M.N., ed., *Electromagnetic Methods in Applied Geophysics*, Vol. 1, Soc. Expl. Geophys., 313-363.
- Lee, K. H., Kim, H. J., and Uchida, T., 2003, Electromagnetic fields in steel-cased borehole, *Geophys. Prosp.* (submitted)
- Newman, G. A., 1995, Crosswell electromagnetic inversion using integral and differential equations, *Geophysics*, **60**, 899-911.
- Parker, R. L., 1994, *Geophysical Inverse Theory*, Princeton Univ. Press.
- Sena, A. G., and Toksoz, M. N., 1990, Simultaneous reconstruction of permittivity and conductivity for crosshole geometries, *Geophysics*, **55**, 1302-1311.
- Tikhonov, A. N., and Arsenin, V. Y., 1977, *Solutions to Ill-Posed Problems*, John Wiley and Sons, Inc.
- Ward, S. H., and Hohmann, G.W., 1988, Electromagnetic theory for geophysical applications, in Nabighian, M.N., ed., *Electromagnetic Methods in Applied Geophysics*, Vol. 1, Soc. Expl. Geophys., 131-311.
- Wilt, M. J., Alumbaugh, D. L., Morrison, H. F., Becker, A., Lee, K. H., and Deszcz-Pan, M., 1995, Crosshole electromagnetic tomography: System design considerations and field results, *Geophysics*, **60**, 871-885.
- Wilt, M. J., Mallan, R., Kasameyer, P., and Kirkendall, B., 2002, Extended 3D induction logging for geothermal resource assessment: Field results with the Geo-BILT system, Proc. 27th Workshop on Geothermal Reservoir Engineering, Stanford Univ., SGP-TR-171.
- Zhdanov, M. S., and Fang, S., 1996, Quasi-linear approximation in 3-D EM modeling, *Geophysics*, **61**, 646-665.
- Zhou, Q., Becker, A., and Morrison, H. F., 1993, Audio-frequency electromagnetic tomography in 2D, *Geophysics*, **58**, 482-495.



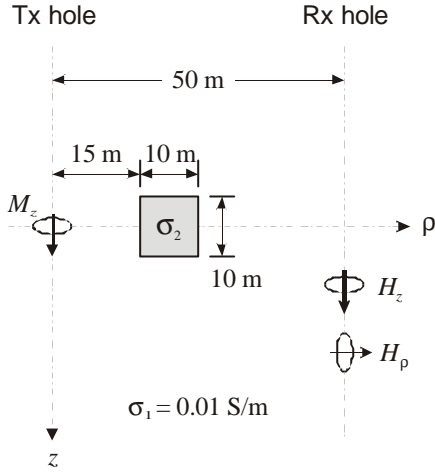


Figure 1. A cylindrically symmetric model. A conductive body with a cross-section of 10 m by 10 m is cylindrically symmetric about a borehole in which vertical magnetic dipole ( $M_z$ ) source is inserted, and located in a whole space of 0.01 S/m at 15 m horizontally away from the borehole. Horizontal and vertical magnetic fields are measured in the other borehole 50 m horizontally away from the source borehole.

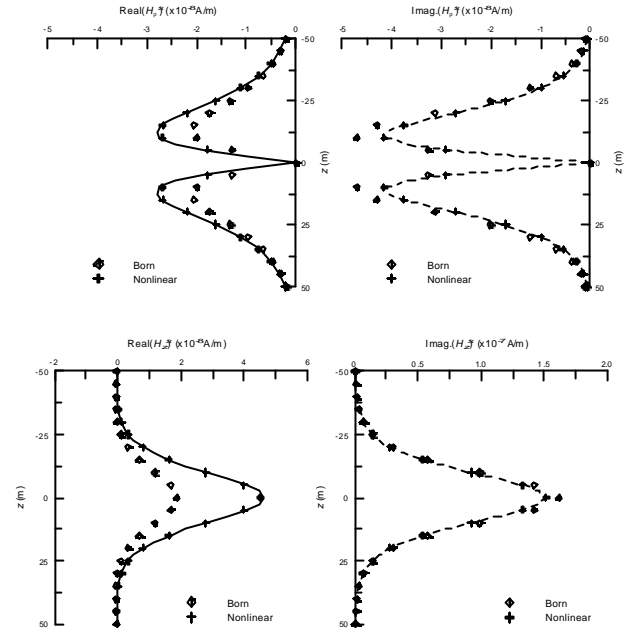


Figure 2. Horizontal (upper) and vertical (lower) components of secondary magnetic fields. Frequency is  $10^4$  Hz and body conductivity is 0.1 S/m. Solid and dashed lines show FE solutions.

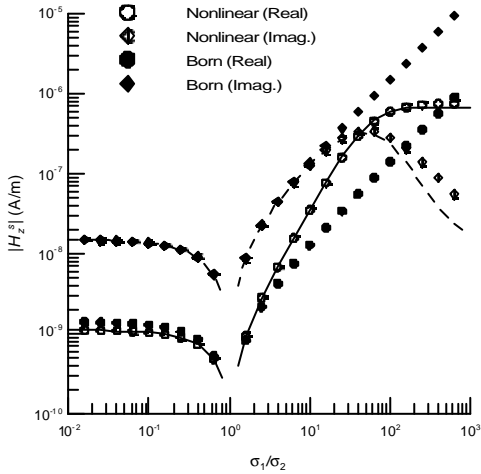


Figure 3. The effect of conductivity contrast between the body and background on the vertical components of secondary magnetic fields. The depths of source and receiver are fixed at 5 m above and below the bottom of the body, respectively. The operating frequency is  $10^4$  Hz. Solid and dashed lines show FE solutions.

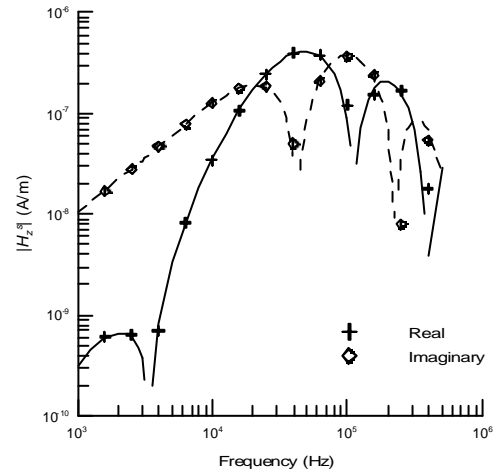


Figure 4. The effect of frequency on the vertical components of secondary magnetic fields. The depths of source and receiver are fixed at 5 m above and below the bottom of the body, respectively. The conductivity of the body is 0.1 S/m. Solid and dashed lines show FE solutions.

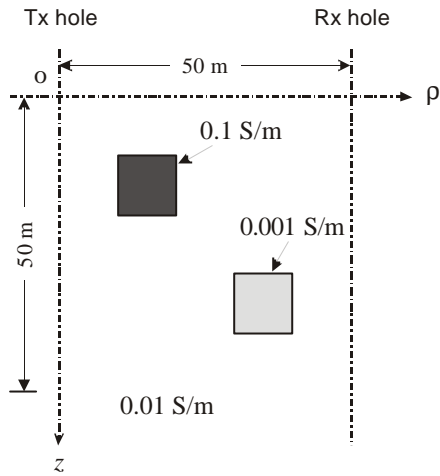


Figure 5. A model used to calculate synthetic data for inversion test. Two bodies of 0.1 S/m and 0.001 S/m, separated vertically by 10 m, are located in a whole-space of 0.01 S/m. The upper conductive and lower resistive ones are at 10 m and 30 m horizontally away from the source borehole, respectively.

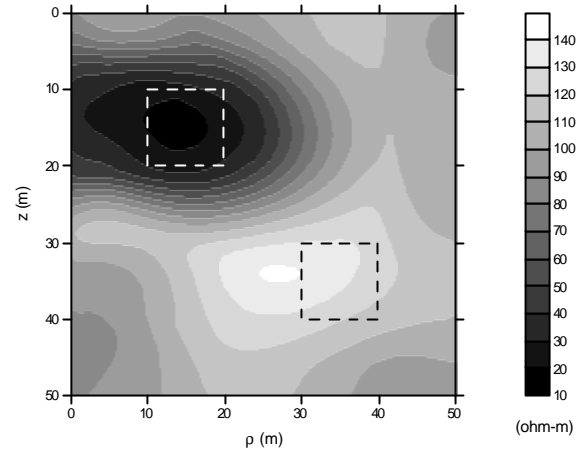


Figure 6. An image of the two conductors reconstructed from the inversion of synthetic data after 8th iteration.

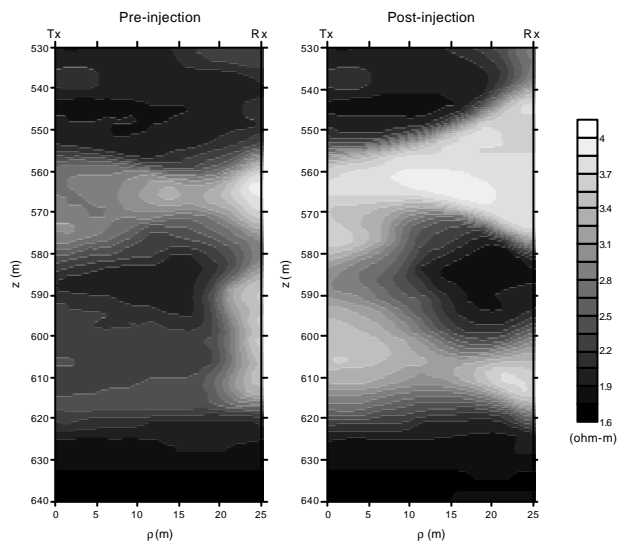


Figure 7. Resistivity imaging derived from the 2-D inversion of data obtained in the Lost Hills CO<sub>2</sub> pilot project in southern California.